

Establishment of the ac electrokinetic elongation mechanism of DNA by three-dimensional fluorescent imaging

C. Wälti, P. Tosch, A. G. Davies, W. A. Germishuizen, and C. F. Kaminski

Citation: *Appl. Phys. Lett.* **88**, 153901 (2006); doi: 10.1063/1.2188587

View online: <http://dx.doi.org/10.1063/1.2188587>

View Table of Contents: <http://apl.aip.org/resource/1/APPLAB/v88/i15>

Published by the AIP Publishing LLC.

Additional information on *Appl. Phys. Lett.*

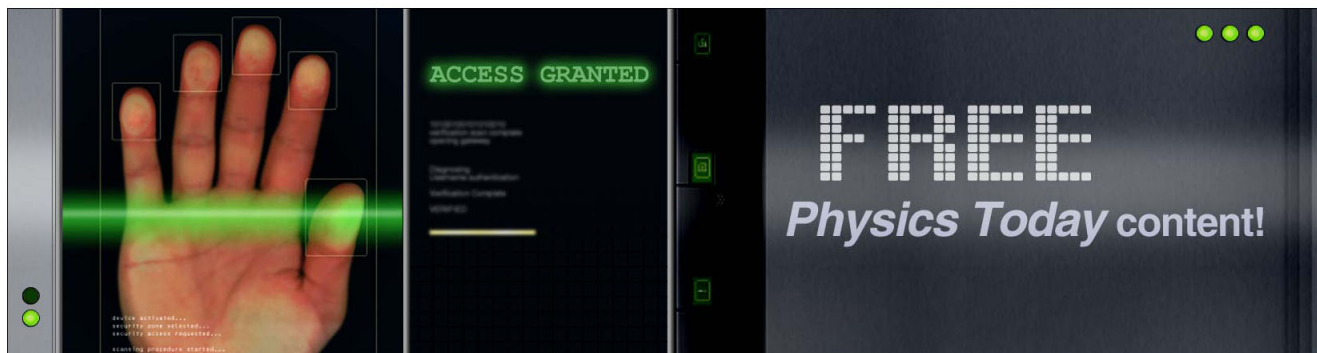
Journal Homepage: <http://apl.aip.org/>

Journal Information: http://apl.aip.org/about/about_the_journal

Top downloads: http://apl.aip.org/features/most_downloaded

Information for Authors: <http://apl.aip.org/authors>

ADVERTISEMENT



Establishment of the ac electrokinetic elongation mechanism of DNA by three-dimensional fluorescent imaging

C. Wälti,^{a)} P. Tosch, and A. G. Davies

School of Electronic and Electrical Engineering, University of Leeds, Leeds, LS2 9JT, United Kingdom

W. A. Germishuizen and C. F. Kaminski

Department of Chemical Engineering, University of Cambridge, Cambridge, CB2 3RA, United Kingdom

(Received 29 July 2005; accepted 26 February 2006; published online 10 April 2006)

We report three-dimensional imaging measurements using confocal microscopy of fluorescently labelled deoxyribonucleic acid (DNA) strands subjected to strong ac electric fields. The DNA molecules are covalently tethered by one end to gold microelectrodes and the observed elongation patterns are compared with the electric field lines obtained from numerical simulations and with previously determined fluid flow patterns. We demonstrate that the major contribution to the elongation stems from the ac electrokinetic torque, supplemented by a small bias force provided by the electric-field-induced fluid flow, and we provide evidence that the observed restricted elongation owing to the geometries of the electrodes results from a sign change in the bias force.

© 2006 American Institute of Physics. [DOI: 10.1063/1.2188587]

For many applications in molecular nanotechnology the ability to manipulate molecules on the molecular scale is essential to control their position and orientation, and hence their efficacy. A number of techniques are used to achieve this, including scanning probe techniques,¹ optical² and magnetic tweezers,³ and movement via hydrodynamic drag forces.⁴ Recently, ac electrokinetic manipulation techniques have received attention and have been used to manipulate particles of various sizes,⁵ and to concentrate^{6,7} and elongate^{8,9} DNA molecules. In many of these studies, the various forces acting on the molecule during the ac electrokinetic manipulation induce a conformational change in the molecule. This fundamental and important feature needs to be well characterized and understood before this manipulation technique can fully realize its potential. This motivates the present study where we investigate the ac-electrokinetic-induced conformational changes of surface tethered molecules.

A number of studies have been performed on ac-electrokinetic-induced conformational changes, in particular on the elongation of long molecules.^{6,9,10} However, the current understanding of the mechanisms responsible for the elongation of polarizable molecules, such as DNA, in strong ac electric fields is far from complete. One possible mechanism for the elongation of surface tethered DNA was proposed in Ref. 11 and discussed in detail in Ref. 9; here, the DNA molecules are modelled as long strings of connected short segments.¹² In an electric field, a dipole is induced in each segment, and the resulting electrokinetic torque aligns the segments with the field. However, the probability of parallel and antiparallel alignment of the segments with the electric field is equal and therefore no elongation is expected in this case. To achieve elongation, an additional bias force, i.e., a point force pulling on the free end of the DNA, is required so that a forward, parallel alignment of the segments is favored over an antiparallel alignment. In principle, this bias force can be provided by the electric field acting on

the induced dipoles of the segments. However, such a dielectrophoretic force would point towards the ends of the molecules that are tethered to the surface and therefore would not result in elongation. Alternatively, since the strong electric fields additionally induce a fluid flow in the solute surrounding the DNA,^{9,13,14} viscous drag could provide the bias force. In fact, the DNA may be entirely elongated by a fluid-flow-induced viscous drag without any electrokinetic contribution on the DNA itself. The roles of the various forces acting on the DNA molecules during elongation remain to be established and more detailed investigations into their interplay, and in particular, between the electrokinetic torque and the induced fluid flow, are required.

Recently, we reported on the elongation of DNA molecules between opposing microelectrodes using ac electric fields and investigated the electric-field-induced fluid flow between the microelectrodes.⁹ As shown schematically in Fig. 1, the pattern of the electric-field-induced fluid flow is different from the electric field lines; in fact, they are nearly perpendicular at the center of the gap between the electrodes. It might therefore be expected that different elongation trajectories will arise from different elongation mechanisms, with any differences being most pronounced around the center of the gap. Top-view two-dimensional (2D) imaging has shown that DNA molecules elongated between electrodes cannot be stretched to beyond the mid-point of the gap, regardless of the molecular length.^{9,15} However, other than providing a bias force, contributions to elongation by the fluid flow might be expected to result in an upturn of the DNA molecules around the midpoint of the gap if the molecules followed the fluid flow pattern (Fig. 1), which cannot be detected by top view 2D imaging.

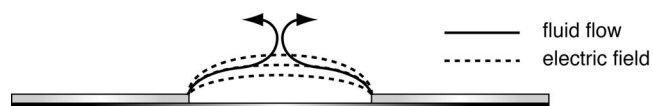


FIG. 1. Schematic view of the electric field lines and the fluid flow pattern (Ref. 9) between two biased microelectrodes.

^{a)} Author to whom correspondence should be addressed; electronic mail: c.walti@leeds.ac.uk

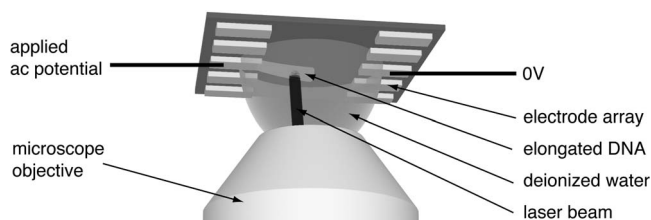


FIG. 2. Schematic diagram of the experimental arrangement.

A better understanding of the elongation mechanism and the interplay between the various forces would therefore be achieved by performing three-dimensional (3D) imaging on such elongation-restricted systems. In this letter, we report imaging measurements using confocal microscopy of fluorescently labelled DNA strands covalently tethered by one end to gold microelectrodes and subjected to strong ac fields. We compare the observed elongation patterns with the electric-field lines obtained from numerical simulations and with previously determined⁹ fluid flow patterns. Electric fields of 600 kV/m at frequencies between 200 kHz and 1 MHz are applied across the 20- μm or 40- μm -wide gaps between two opposing electrodes. We show that the contour of the area containing the DNA resembles the shape of the electric-field lines regardless of the direction of the fluid flow for all frequencies and lengths of DNA investigated.

The microelectrode array comprised two opposing rows of individually addressable electrodes, 30 μm wide, and 15 μm apart (Fig. 2). The rows were separated by either by a 20- μm or 40- μm -wide gap. The electrodes (20 nm NiCr, 80 nm Au) were formed on Si/SiO₂ wafers using standard optical lithography techniques. The wafers were glued and bonded into a chip package and cleaned in “piranha” solution (H₂O₂:H₂SO₄, 3:7 ratio) for 1 h.

λ -DNA [48,502 basepairs (bp), Sigma-Aldrich] was used in all experiments. The procedure for tethering DNA onto the surface via one end is described in detail in Ref. 8. Before immobilization, the DNA was diluted to 50 ng/ μl in TE (10 mM tris-HCl, 1 mM EDTA, pH 8) 1 M NaCl solution, and the fluorescent intercalator YOYO-1 (excitation/emission wavelength 488/515 nm, Molecular Probes) was added at an intercalator to basepair ratio of 1:8. The contour length of λ -DNA at the YOYO-1 concentration used in this work increases to approximately 20 μm .⁹

For all elongation experiments, the wafers were submerged in deionized water (conductivity $\sim 10^{-5}$ S/m). The ac electric fields were generated by applying an ac potential to the chosen electrode while grounding the electrode directly opposite. All other electrodes were left at floating potential during the experiments. Electric-field values referred to in this work are the amplitude of the applied potential divided by width of the gap between opposing electrodes.

The elongation of surface tethered DNA molecules was studied with a confocal laser scanning microscope (Olympus, FV300/IX70) using a 60 \times water immersion lens. The fluorescently labelled DNA molecules were excited by the 488 nm line of a 20 mW argon-ion laser, and the emitted light was collected behind a combination of a 510 nm long-pass and 515 nm bandpass filter. 3D images were acquired by imaging multiple x - y planes at different z heights, using a 0.2 μm -step-size in the z -direction and were processed with the Huygens Essential software package (SVI).

We modeled the electric field around the electrodes using the finite element analysis software FEMLAB (Comsol).

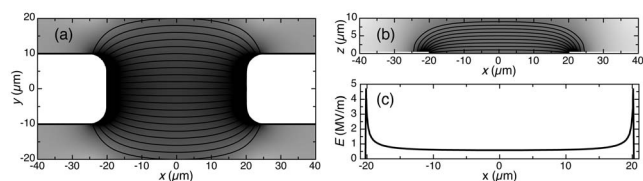


FIG. 3. Modeling of the electric field between two opposing electrodes separated by 40 μm . The left electrode was set to 30 V while the right electrode was set to 0 V for the modeling. (a) and (b) Side view (x - z) and top view (x - y) of the electrode arrangement, respectively; the grey scale indicates the field strength with white being 0 V/m and black 1 MV/m. (c) Electric-field values between two opposing electrodes at the top surface of the electrodes as a function of distance from the center of the gap.

For the model, the electrodes were represented by a 100-nm-thick layer of gold, separated by gaps of either 20 μm or 40 μm , suspended in a medium with a conductivity of 10^{-5} S/m; the results are shown in Fig. 3. As expected, the electric field is highest directly at the electrode edge and goes through a minimum at the center of the gap; however, the variation of the field is small across most of the gap and so we can assume that the elongated DNA molecules experience similar field strengths over most of the gap.

The elongation is a function of frequency and amplitude of the applied ac field.⁹ The elongation is almost negligible for frequencies below 100 kHz, but increases with frequency to reach a maximum at around 250 kHz. For higher frequencies, the amount of elongation decreases and we were not able to detect any elongation above 1 MHz.⁹ We imaged the elongated DNA in an applied field of 600 kV/m at several frequencies across a 40- μm gap and Fig. 4(a) shows the results at 210 kHz in an x - z and x - y cross section. The DNA is visible as a fluorescent band extending from the edge of the left electrode. From the side view, it can be seen that the DNA extends at a range of angles with respect to the wafer plane. The length of the elongated DNA is about 20 μm across the 40- μm gap, demonstrating that full elongation is possible under these conditions.

Figure 4(b) shows the side views of the same measurements at higher frequencies. As expected, the length of the elongated DNA decreases with increasing frequency, and is almost undetectable at 1 MHz. The measured lengths of elongation are in good agreement with Ref. 9 for a similar experimental arrangement. Regardless of the frequency of the applied field and thus the degree of elongation, the elongated molecules follow the same elongation pattern as in Fig. 4(a) for the fully elongated situation. If we compare the elongation pattern of the DNA molecules with the calculated electric-field lines, it is apparent that the contour of the area containing the DNA molecules resembles the shape of electric field over the whole length of the DNA [Fig. 4(c)]. These findings indicate that the electrokinetic torque acting on the DNA molecules by aligning the individual segments with the field lines contributes substantially to the elongation of the molecules. However, to understand better the situation at the center of the gap, the gap has to be sufficiently small that the elongation of the DNA is restricted.

Reducing the electrode separation to less than twice the DNA contour length reduces the maximum elongation length since the DNA molecules cannot be elongated beyond the mid-point of the gap.⁹ Figure 5(a) shows the side-views of the elongation of λ -DNA molecules in ac electric fields of 600 kV/m at different frequencies across a 20- μm -wide gap.

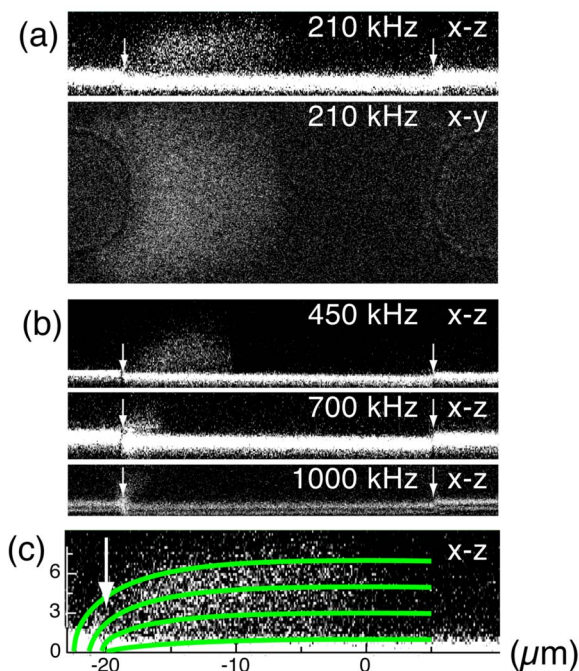


FIG. 4. (Color online) λ -DNA elongated across 40- μ m-wide gaps. The white arrows indicate the edges of the electrodes. (a) Side (x - z) and top (x - y) view at 210 kHz. (b) Side views at 450 kHz, 700 kHz, and 1000 kHz. (c) Side view at 210 kHz overlaid with calculated electric-field lines (green).

As in the 40- μ m-gap case, the elongation is largest at 210 kHz and decreases with increasing frequency. However, even at 210 kHz, elongation is only about 10 μ m, corresponding to one-half of the distance between the electrodes. For all frequencies investigated, the DNA molecules follow the same elongation pattern. Figure 5(b) compares the curvature of the elongation with the calculated electric-field lines. Although the elongation is restricted to one-half of the gap width, the contour of the area containing the DNA molecules still resembles the shape of the electric field lines even at the center of the gap.

As discussed above, the ac electric field not only acts on the induced dipoles in the DNA, but also induces a fluid flow directed inwards from the electrodes toward the center of the gap, where it changes direction and becomes vertical, away from the wafer (see Fig. 1).⁹ If the fluid flow, and thus the resulting viscous drag, were a major contribution to the elongation mechanism, the DNA molecules would be expected to follow the fluid flow pattern. Figure 5(b) compares the curvature of the elongation with the fluid flow pattern obtained from Ref. 9 and suggests that the DNA does not follow the fluid flow as there is no sign of an upturn at the center of the gap, although in Fig. 5(b) the DNA molecules are only extended to about half of their full contour length. This, together with the fact that the contour of the area containing the elongated DNA follows the pattern of the electric field when elongated regardless of amplitude and frequency, supports the model of elongation proposed in Refs. 9 and 11 that the fluid flow does not play a dominant role in the elongation. However, in this model, elongation only results if there is a finite effective bias force parallel to the electric field lines. We propose that this is provided by the fluid flow since in the center of the gap, the effective bias force is zero and is of opposite direction beyond the center, and therefore no elongation is possible across the gap, in agreement with our experimental findings.

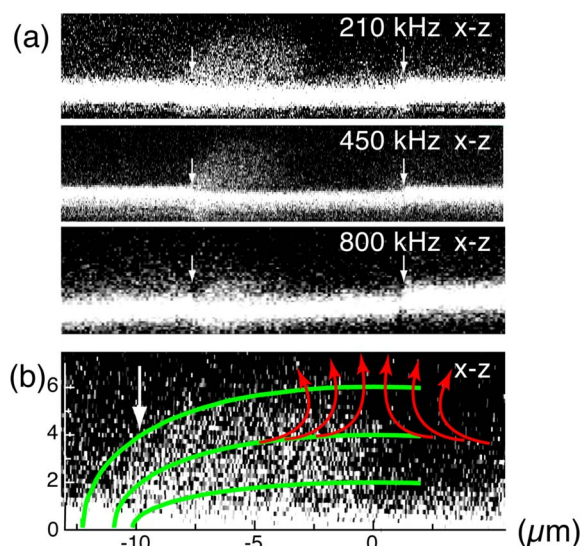


FIG. 5. (Color online) λ -DNA elongated across 20- μ m-wide gaps. The white arrows indicate the edges of the left and right electrodes. (a) Side views at 210 kHz, 450 kHz, and 800 kHz. (b) Side view at 210 kHz overlaid with calculated electric-field lines (green). The red arrows in the center of the gap show an indicative trajectory of the fluid flow.

In conclusion, we investigated the elongation of λ -DNA by ac electric fields using 3D optical imaging techniques. We presented evidence for a mechanism where the main contribution to the elongation is via the electrokinetic torque supplemented by a bias force provided by the component of the electric-field-induced fluid flow parallel to the electric field lines.

This research was in part funded by the EPSRC.

- ¹W. Bowen, R. W. Lovitt, and C. Wright, *Biotechnol. Lett.* **22**, 893 (2000); E. Florin, V. Moy, and H. Gaub, *Science* **264**, 415 (1994); H. G. Hansma, *Annu. Rev. Phys. Chem.* **52**, 71 (2001).
- ²M. D. Wang, H. Yin, R. Landick, J. Gelles, and S. M. Block, *Biophys. J.* **72**, 1335 (1997); C. Bustamante, Z. Bryant, and S. B. Smith, *Nature (London)* **421**, 423 (2003).
- ³F. Amblard, B. Yurke, A. Pargellis, and S. Leibler, *Rev. Sci. Instrum.* **67**, 1 (1996); C. Haber and D. Wirtz, *Rev. Sci. Instrum.* **71**, 4561 (2000); T. R. Strick, J. F. Allemand, V. Croquette, and D. Bensimon, *J. Stat. Phys.* **93**, 647 (1998).
- ⁴T. T. Perkins, D. E. Smith, R. G. Larson, and S. Chu, *Science* **268**, 83 (1995); S. Smith, L. Finzi, and C. Bustamante, *Science* **258**, 1122 (1992); R. Zimmermann and E. Cox, *Nucleic Acids Res.* **22**, 492 (1994).
- ⁵J. Gimsa, *Bioelectrochemistry* **54**, 23 (2001); J. Suehiro and R. Pethig, *J. Phys. D* **31**, 3298 (1998); H. Morgan and N. G. Green, *J. Electrostat.* **42**, 279 (1997).
- ⁶C. L. Asbury, A. H. Diercks, and G. Van der Engh, *Electrophoresis* **23**, 2658 (2002).
- ⁷M. Washizu, S. Suzuki, O. Kurosawa, and T. Nishizaka, *IEEE Trans. Ind. Appl.* **30**, 835 (1994).
- ⁸W. A. Germishuizen, C. Wälti, R. Wirtz, M. B. Johnston, M. Pepper, A. G. Davies, and A. P. J. Middelberg, *Nanotechnology* **14**, 896 (2003).
- ⁹W. A. Germishuizen, P. Tosch, A. P. J. Middelberg, C. Wälti, A. G. Davies, R. Wirtz, and M. Pepper, *J. Appl. Phys.* **97**, 014702 (2005).
- ¹⁰S. Suzuki, T. Yamanashi, S. Tazawa, O. Kurosawa, and M. Washizu, *IEEE Trans. Ind. Appl.* **34**, 75 (1998).
- ¹¹A. E. Cohen, *Phys. Rev. Lett.* **91**, 235506 (2003).
- ¹²J. F. Marko and E. D. Siggia, *Macromolecules* **28**, 8759 (1995).
- ¹³N. G. Green, A. Ramos, and H. Morgan, *J. Phys. D* **33**, 632 (2000).
- ¹⁴H. Morgan and N. G. Green, *AC Electrokinetics: Colloids and Nanoparticles* (Research Studies, Baldock, Hertfordshire, UK, 2003).
- ¹⁵W. A. Germishuizen, C. Wälti, P. Tosch, R. Wirtz, M. Pepper, A. G. Davies, and A. P. J. Middelberg, *IEE Proc., Nanobiotechnol.* **150**, 54 (2003).